Journal of Molecular Histology
https://doi.org/10.1007/s10735-020-09913-5

ORIGINAL PAPER

Hedgehog pathway activation in oral squamous cell carcinoma: cancer-associated fibroblasts exhibit nuclear GLI-1 localization

Vanessa Sousa Nazare Guimaraes[1,2] · Manuela Torres Andion Vidal[1,2] · Ludmila de Faro Valverde[1,2] · Marbele Guimarães de Oliveira[1,2] · Leonardo de Oliveira Siquara da Rocha[1,2] · Paulo Lucas Cerqueira Coelho[1] · Fernando Augusto Soares[3,4] · Bruno Solano de Freitas Souza[1] · Daniel Pereira Bezerra[1] · Ricardo D. Coletta[5] · Thiago Almeida Pereira[6] · Jean Nunes dos Santos[2] · Clarissa Araújo Gurgel Rocha[1,2,7]

Received: 29 April 2020 / Accepted: 22 September 2020

Abstract

The purpose of this study was to evaluate the expression of Hedgehog (HH) signaling molecules (SHH and GLI-1) by cancer-associated fibroblasts (CAF) in oral squamous cell carcinoma (OSCC). Immunohistochemistry was used to detect molecular HH signaling and CAF-related protein expression, including α-SMA and S100A4, in 70 samples of human OSCC. The colocalization of α-SMA and S100A4 with SHH was also evaluated by double-staining. In vitro study was performed using primary normal oral fibroblast (NOF) and CAF through immunofluorescence and Western Blot for CAF-proteins, SHH, and GLI-1. Forty-five cases (64.28%) were positive for α-SMA exclusively in tumor stroma, and S100A4 was identified in the cytoplasm of CAFs in 94.28% (n = 66) of the cases. With respect to stromal cells, 64 (91.43%) OSCC cases were positive for SHH, and 31 were positive for GLI-1 (44.29%); positive correlations were found between SHH and α-SMA ($p < 0.0001$, $\varphi = 0.51$), as well as between SHH and S100A4 ($p = 0.087$, $\varphi = 0.94$). Protein expression of SHH and GLI-1 was observed in primary CAFs and NOFs. Although SHH was found to be localized in the cellular cytoplasm of both cell types, GLI-1 was present only in the nuclei of CAF. Our results indicate that CAFs are not only potential sources of HH ligands in tumor stroma, but may also respond to HH signaling through nuclear GLI-1 activation. We further observed that elevated SHH expression by OSCC cells was associated with higher CAF density, reinforcing the chemoattractant role played by these molecules.

Keywords Oral cancer · Cancer-associated fibroblast · GLI1 protein · Hedgehog protein

Introduction

Oral squamous cell carcinoma (OSCC) is a locally invasive tumor frequently diagnosed at advanced clinical stages, with an approximately 50% mortality rate (Adrien et al. 2014; Chi et al. 2015). More than 350,000 people are affected

Electronic supplementary material The online version of this article (https://doi.org/10.1007/s10735-020-09913-5) contains supplementary material, which is available to authorized users.

✉ Clarissa Araújo Gurgel Rocha
clarissa.gurgel@fiocruz.br; clarissagurgelrocha@gmail.com

[1] Gonçalo Moniz Institute, Oswaldo Cruz Foundation, Waldemar Falcao Street, 121, Candeal, Salvador, Bahia 40296-710, Brazil

[2] Federal University of Bahia, Augusto Viana Street, s/n, Canela, Salvador, Bahia 40110-909, Brazil

[3] D'Or Institute for Research and Education, Diniz Cordeiro Street, 30, Botafogo, Rio de Janeiro 22281-100, Brazil

[4] School of Dentistry, University of São Paulo, Prof. Almeida Prado Avenue, 1280, Butantã, São Paulo 05508-900, Brazil

[5] School of Dentistry, University of Campinas, Limeira Avenue, 901, Areiao, Piracicaba, São Paulo 13414-903, Brazil

[6] Institute for Stem Cell Biology and Regenerative Medicine, Stanford University School of Medicine, 265 Campus Drive, Stanford, CA 94305-5463, USA

[7] Laboratory of Pathology and Molecular Biology, Gonçalo Moniz Institute, Oswaldo Cruz Foundation,121 Waldemar Falcao, Candeal, Salvador, Bahia, Brazil

Published online: 30 September 2020

worldwide (Bray et al. 2018) each year, especially smokers aged 50–60 years (Chi et al. 2015).

The pathogenesis of OSCC is complex and involves mutations in groups of genes primarily involved in cell cycle regulation (Ansari et al. 2018). A recent large-scale mutational analysis of 203 OSCC cases (located on the tongue and floor of the mouth), available from TCGA (https://www.cbioportal.org), revealed that mutations in TP53 and CDKN2A were present in more than 70% and 50% of these cases, respectively (Cerami et al. 2012; Gao et al. 2013). Moreover, network analyses of interactions occurring between the signaling networks mainly involved in OSCC pathogenesis have revealed that, despite mutations being uncommon among the Hedgehog pathway genes (SHH, IHH, PTCH1, SMO, and GLI-1), the expression of these HH proteins is directly affected by mutations in p63 and CDKN2A, which are regulated by TP53 (Fig. 1) (Cerami et al. 2012; Gao et al. 2013). Since 2011, due to its importance in squamous cell carcinomas at other sites, such as the lung (Abe and Tanaka 2016) and basal cell carcinoma (Otsuka et al. 2015), the role of the HH pathway in OSCC has been widely studied.

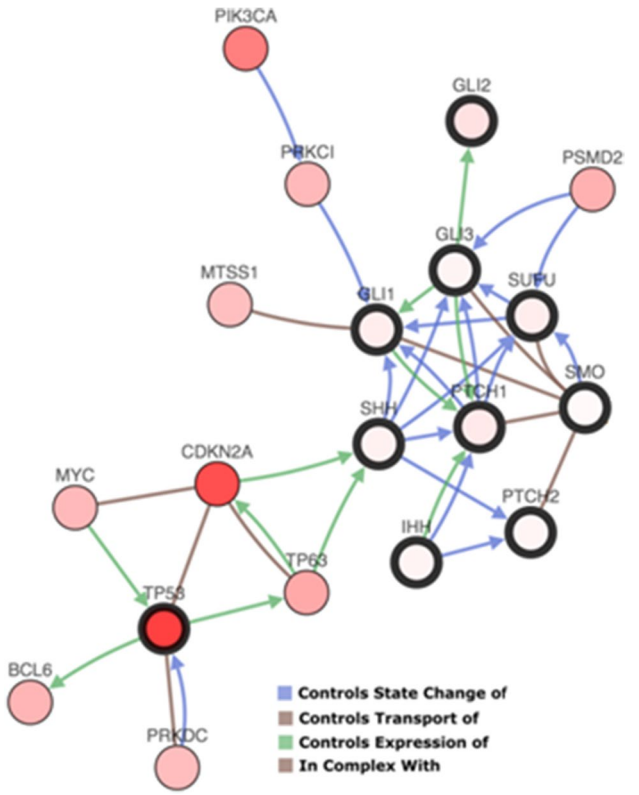

Fig. 1 Main networks involved in OSCC pathogenesis. Shades of red are indicative of mutation frequencies (a darker color indicates a higher frequency of mutation). Mutations in CDKN2A and TP63 frequently occur in OSCC, and both control the expression of the SHH ligand. In addition, GLI-1 expression is controlled by multiple molecules involved in OSCC pathogenesis. (Color figure online)

Importantly, our group demonstrated that the Hedgehog (HH) cascade becomes reactivated in OSCC (Cavicchioli Buim et al. 2011).

The canonical activation of the Hedgehog pathway is known to be mediated by the SHH, IHH and/or DHH ligands. The binding of HH ligands to Ptch induces endocytation and permits Smo to migrate to the tips of primary cilia, where it inhibits the PKA, GSK3, and CSK kinases, promoting GLI-1, 2, and 3 activation. In the nucleus, GLI^A activates genes that contribute to tumor self-renovation (Nayak et al. 2017), angiogenesis (Kuroda et al. 2017), and tumoral stroma activation (Valverde et al. 2016). In the absence of HH-ligands, Gli proteins undergo phosphorylation by several kinases (PKA, GSK3, CSK), becoming ubiquitinated and targeted by the proteasome, in which GLI-1 and -2 are degraded and GLI-3 is processed to become a repressor (GliR); this glioma-like protein then migrates to the nucleus and represses HH-regulated genes (Habib and O'Shaughnessy 2016).

For decades, malignant epithelial cells have been a major focus of cancer studies. However, in recent years, the tumor microenvironment/stroma has been featured as an important functional compartment in tumor biology, since this is where malignant cells interact with genetically unaltered cells, such as fibroblasts, endothelial cells, and macrophages. Among these, cancer-associated fibroblasts (CAF) represent the most abundant cellular subtype within the stroma of several types of tumors (Hanahan and Coussens 2012).

CAFs originate from a variety of precursor cells (Göritz et al. 2011; Jotzu et al. 2011; Quante et al. 2011; Kidd et al. 2012; Gascard and Tlsty 2016), which is reflected by their expression of distinct biomarkers (e.g. α-SMA and S100A4) and, consequently, in the heterogeneity seen in CAF populations (Lin et al. 2017). Among these markers, the detection of α-SMA protein has been a main strategy for identifying CAFs with a myofibroblastic signature (Kellermann et al. 2008; Gascard and Tlsty 2016; Lin et al. 2017), while S100A4 expressing fibroblasts play a distinctively tumor-protective role in immune surveillance through collagen production, and may be a precursor of quiescently activated fibroblasts (Öhlund et al. 2014; Gascard and Tlsty 2016).

The role of CAFs in OSCC pathogenesis and progression has been widely investigated. It has been demonstrated that OSCC tumor cells can promote CAF activation (Kellermann et al. 2008), for instance, through TGF-β1 (Kellermann et al. 2008; Costea et al. 2013), which in turn contributes to tumorigenesis through CAF production of mitogens (Sobral et al. 2011) and other factors that promote angiogenesis (Kayamori et al. 2016), tumor invasion (Costea et al. 2013), epithelial-mesenchymal transition (Cirillo et al. 2017), immunosuppression and immune escape (Takahashi et al. 2017). More importantly, a recent systematic review and metanalysis revealed that higher CAF densities are

frequently associated with parameters indicative of a worse prognosis, including advanced stages of disease, tumor recurrence, depth of invasion, vascular, lymphatic, and neural invasion, extranodal metastatic spread, and an overall decrease in survival (Dourado et al. 2019).

It was recently demonstrated that the HH pathway plays an important role in CAF activation (Bailey et al. 2008; Öhlund et al. 2014; Gascard and Tlsty 2016; Valenti et al. 2017) and that these cells are an important source of SHH (Spivak-Kroizman et al. 2013; Peiris-Pagès et al. 2015). In addition, CAF-mediated paracrine HH pathway activation in tumor cells can support cancer progression (Theunissen and De Sauvage 2009; Abe and Tanaka 2016). Considering the participation of the HH pathway in OSCC pathogenesis, together with the fact that CAFs can mediate and/or respond to the activation of this pathway, the present study endeavored to investigate the molecular immunoexpression of the HH pathway components SHH and GLI-1 in OSCC, notably in CAFs in vitro.

Materials and methods

Human samples

A total of 70 formalin-fixed and paraffin-embedded (FFPE) samples from patients, diagnosed with OSCC and archived at the Pires Diagnostic Center (Feira de Santana, Bahia, Brazil), were included in the study. Tumor-free adjacent margins (TFM) were available in 10 cases of OSCC and were also included in the analysis. All samples were subsequently reviewed and classified by two experienced pathologists according to the WHO histological grading scale (2018) (IARC 2005). The clinical parameters of the patients included in the study are listed in Supplementary Table S1. The present study was conducted in accordance with the Declaration of Helsinki (2013) (The World Health Organization 2001), and permission concerning formalin-fixed and paraffin-embedded samples was granted by the responsible authorities from Pires Diagnostic Center and was approved by the Institutional Ethics Review Board of the Gonçalo Moniz Institute/Oswaldo Cruz Foundation (Approval Protocol no. 2.295.634/CAAE 68,095,016.1.0000.0040).

Immunohistochemistry

Histological sections were stained with H&E (hematoxylin and eosin) for general histology. Immunohistochemistry was performed in serial Sects. (4 µm) after standard dewaxing/rehydrating protocols and heat-induced epitope retrieval in a hot water bath (98 °C) for 45 min. Endogenous peroxidase blocking (Peroxidase Blocking Solution, Dako, Carpinteria, USA) was performed for 10 min, followed by protein blocking with 10% non-fat milk for 30 min. The α-SMA primary antibody was incubated for 1 h at room temperature, and S100A4, FAP, SHH, and GLI-1 primary antibodies were incubated for 18 h at 4 °C. For negative controls, sections were incubated with the same isotype at identical protein concentrations as the primary antibody. The antibody catalog numbers, clones, and dilutions used herein are summarized in Table 1. After washing with PBS, all sections were incubated with Advance™ HRP Link for 20 min, and then subjected to another round of PBS washing followed by incubation with Advance™ HRP Enzyme (Dako Corporation, Carpinteria, USA) for 20 min. Chemical reactions were developed with 3,3-diaminobenzidine (DAB) (Dako, Carpinteria, USA) and all sections were counterstained with Harris hematoxylin.

Immunohistochemical double-staining was performed with the SHH antibody and α-SMA or S100A4 antibodies using the EnVision G2 Doublestain System (Dako, Carpinteria, USA) with Permanent Red and Vina Green chromogens in accordance with manufacturer instructions.

Slides were scanned by an Aperio digital microscope (Leica Microsystems, Wetzlar, Germany) and imaged using Aperio Image Scope software (Leica Microsystems, Wetzlar, Germany). Five representative fields/sample (200x), in which tumor areas with approximately 40% of stroma were present, were selected by a single experienced pathologist (Examiner 1). All immunomarkers were analyzed within these same selected fields. A second experienced pathologist (Examiner 2) analyzed immunostaining for α-SMA, S100A4, SHH, and GLI-1 proteins. For this analysis, the following localization of proteins was also considered: cytoplasmic and/or nuclear (GLI-1) and membrane and/or cytoplasmic (α-SMA, S100A4, SHH). The number of positive cells was divided by the total numbers cells, and the following semi-quantification criteria were applied as

Table 1 Primary antibody clones

Antibody	Commercial brand	Clone	Dilution: IHC	Dilution:WB	Dilution: IF
SHH	Novus Biologicals	5H4	1:1000	1:2000	1:500
GLI 1	Novus Biologicals	Polyclonal	1:600	1:500	1:600
α-SMA	DAKO	1A4	1:200	1:300	1:200
S100A4	DAKO	polyclonal	1:1000	1:500	1:1000

Commercial brand information and dilutions

follows: negative score (−), < 5% of immunolabeled cells; score 1 +, 5–25%; score 2 +, 26–50%; score 3 +, > 51% of positive cells. These same criteria were used for the analysis of TFM.

Primary human cell cultures

Normal oral fibroblast (NOF) and CAF primary cells were established using tissue explants, then isolated and characterized as previously described (Dourado et al. 2019). Briefly, cells were cultivated in Dulbecco's modified Eagle medium (DMEM) (Thermo Fisher Scientific, Waltham, MA, USA) supplemented with 10% bovine fetal serum (Thermo Fisher Scientific, Waltham, MA, USA) and 50 µg/mL of gentamicin (Novafarma, Anápolis, GO, Brazil) for up to 12 passages at 37 °C under 5% CO_2 in an atmospheric incubator. Cells were routinely tested for mycoplasma contamination using MycoAlert Plus (Sigma-Aldrich, St Louis, MO, USA). CAF phenotype maintenance was evaluated after each two passages by immunofluorescence labeling for the α-SMA antibody.

Immunofluorescence

Primary cells (CAF and NOF) were characterized for α-SMA, S100A4, SHH, and GLI-1 proteins by immunofluorescence (Table 1). Cells were plated on cell culture slides (CELLview™, Greiner Bio-One, Germany) at a density of 0.7×10^5 cells/mL. All cultures were rinsed three times with PBS (pH 7.4) and fixed with 4% paraformaldehyde for 20 min at 0ºC. The excess paraformaldehyde was discarded, and all plates were allowed to dry at room temperature. Following rehydration with PBS and permeabilization with PBS-Triton, the non-specific binding of antibody reagents was blocked by pre-incubating culture plates with 3% bovine serum albumin (BSA) in PBS. Next, the cultures were incubated with the same antibodies listed in Table 1, diluted in PBS/BSA (1%) in a humid chamber at 4ºC overnight.

The following day, all cells were rinsed three times with PBS and the following secondary antibodies were added: Alexa Fluor 568 red goat anti-mouse IgG (1:500, Molecular Probes Eugene, Oregon, USA) and Alexa Fluor 488 green goat anti-rabbit IgG (1:500, Molecular Probes Eugene, Oregon, USA). These antibodies were diluted in PBS and incubated under slow stirring for 1 h at room temperature. Control immunostaining was performed by incubating cultures exclusively with the secondary antibodies.

Finally, nuclear chromatin was stained with 4′, 6-diamidino-2-phenylindole (DAPI) (Molecular Probes, Eugene, Oregon, USA) at a concentration of 5 mg/mL for 10 min at room temperature. All cultures were washed three times with PBS and cells were mounted on slides containing n-Propyl Gallate, an anti-fading agent. A confocal microscope (Confocal Leica SP8, Leica Microsystems Wetzlar, Germany) was used for analysis. All experiments were performed in triplicate.

Western blot

For protein quantification, cells were harvested, washed with PBS and lysed with 50 mMTris–HCl pH 7.4 buffer containing 1% Triton X-100, 150 mM, NaCl, 0.5 mM EGTA and 0.5 mM EDTA, as well as an anti-protease cocktail (Complete Protease inhibitor Cocktail Tablets, Roche, France). Fresh protein extracts from two replicates (30 µg each one) were pooled and separated by SDS-PAGE and transferred to Hybond-C Extra nitrocellulose membranes (GE Healthcare, USA).

The same antibodies described in Table 1 were also used for immunoblotting, the following secondary antibodies were added for Western blotting: anti-mouse IgG (Santa Cruz Biotechnology, 1:10,000), anti-rabbit IgG (GE Healthcare, 1:10,000) and anti-goat IgG (Santa Cruz Biotechnology, 1:10,000). Signals were detected using Enhanced Chemiluminescence (ECL) reagents (PerkinElmer, France). Densitometric analysis was achieved using ImageJ software (National Institutes of Health).

Statistical analysis

Scoring results from the semi-quantitative analysis were analyzed by 3 × 3 chi-square tests and φ (Phi) correlation using SPSS software version 17.0 (SPSS, Inc, Chicago, IL, USA). The value of "p" corresponding to alpha (α) less than or equal to 5% was considered significant, while a value of φ > 0.5 was adopted to indicate a strong positive association, in accordance with Davis (1971).

Results

Heterogeneity of CAF population in OSCC

The α-SMA protein was diffusely distributed in 45 of the OSCC cases (64.28%), and identified exclusively in the membranes and cytoplasm of those stromal cells morphologically similar to fibroblasts located adjacent to tumor islets, with a predominant score of 3 + (n = 24, 53.33%). Positivity for the S100A4 protein was also seen in fibroblasts (3 + score: n = 41, 62.13%), and focal positivity was observed in endothelial, inflammatory and malignant cells (1 + score: n = 34, 66.67%). Remaining scores are described in Table 2. While all TFMs were negative for α-SMA, immunostaining for S100A4 was observed in 90% (n = 9) of the stromal cells in the TFMs included in the study (3 + score: n = 4; 44.44%). Figure 2 illustrates the immunostaining patterns found for α-SMA and S100A4 in OSCC tumor stroma

Table 2 Immunostaining score for tumors cells and stromal cells

Immunohistochemical expression of proteins																
	Tumor cells								Stromal cells							
	0		1+		2+		3+		0		1+		2+		3+	
	n	%	n	%	n	%	n	%	n	%	n	%	n	%	n	%
α-SMA	70	100	0	0	0	0	0	0	25	35.72	13	18.58	8	11.42	24	34.28
S100A4	19	27.14	34	48.58	13	18.58	4	5.7	4	5.72	8	11.42	17	24.28	41	58.58
SHH	6	8.57	8	11.43	6	8.57	50	71.43	31	44.28	23	32.86	8	11.43	8	11.43
GLI1	15	21.42	15	21.42	12	17.16	28	40	39	55.71	23	32.86	7	10	1	1.43

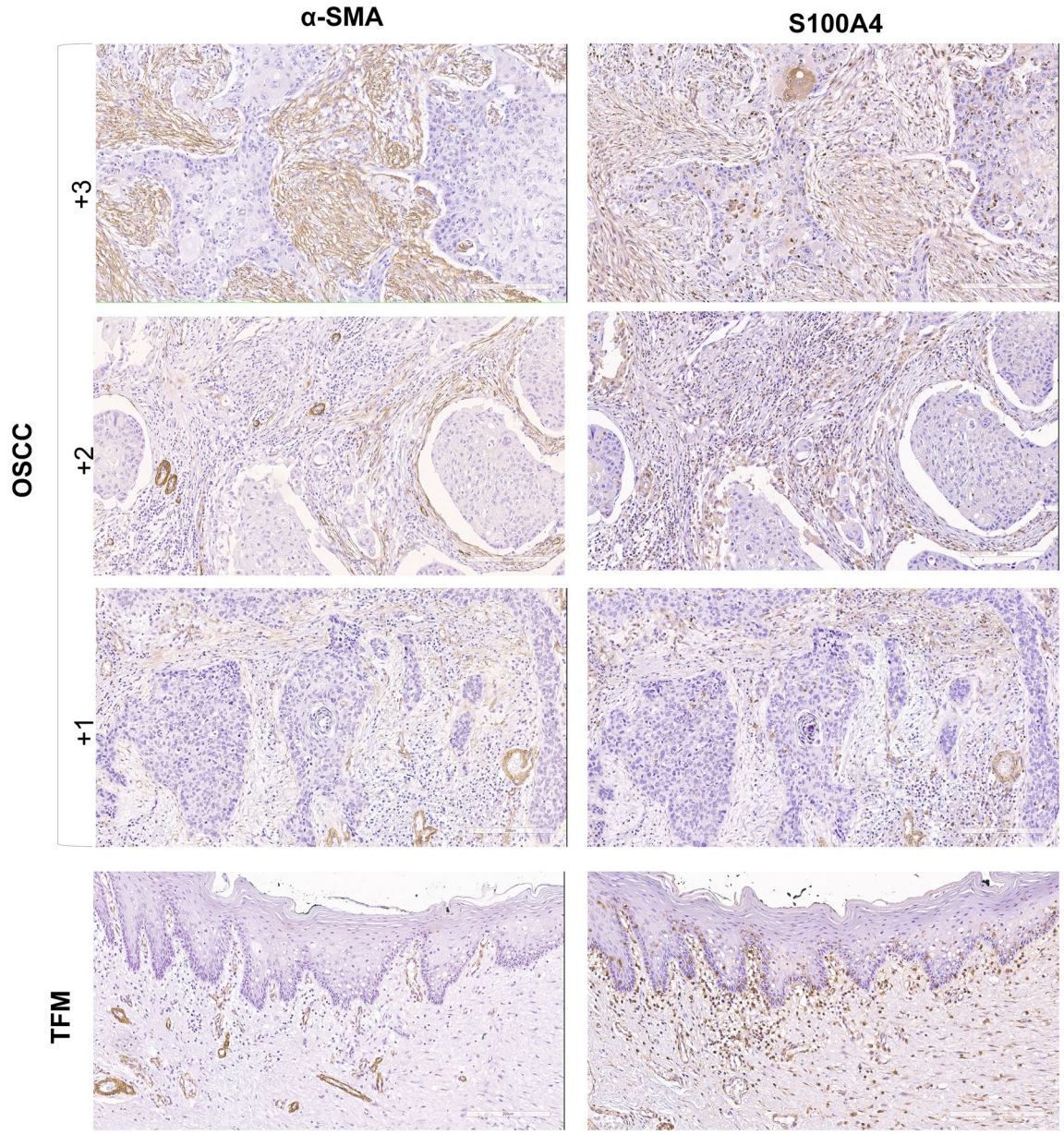

Fig. 2 Immunomarkers expressed by CAFs in OSCC and TFM. All analyses were performed in identical fields. Diffuse and abundant immunostaining for α-SMA and S100A4 (3+score) in tumor stroma. Some positive (1+score) malignant cells are evident. Localized immunostaining for α-SMA and S100A4 (2+score) in OSCC stroma. α-SMA and S100A4 (1+score) in tumor stroma. α-SMA positivity observed exclusively in vessels in TFM. Sparse S100A4 expression observed in the lamina propria of TFM. (Color figure online)

and CAFs in TFMs. A positive correlation between α-SMA and S100A4 ($p < 0.0001$, $\varphi = 0.24$) was observed only in OSCC tumor stroma, but not in TFMs.

Stromal cells and malignant cells express the sonic hedgehog ligand and the HH target gene GLI-1 in OSCC

SHH was detected in the cytoplasm of fibroblasts (SHH: n = 39, 55.72%) with a predominant score of 1 +. Immunopositivity for this protein was also seen in the cytoplasm of malignant cells in 91.43% (n = 64) of the OSCC cases, respectively, with a corresponding score of 3 + (n = 50, 78.13%). With respect to the GLI-1 protein, although cytoplasmic and nuclear immunostaining was seen in fibroblasts (n = 31; 44.29%), this was more frequent in tumor cells, with a predominant score of 1 + (n = 23; 74,20). The remaining scores are described in Table 2. In all TFMs, fibroblasts in the lamina propria presented cytoplasmic positivity for SHH, while epithelial cells were positive for SHH in 60% of the OSCC cases (n = 6) (Fig. 3).

Although positivity for SHH was also identified in both α-SMA and S100A4 positive fibroblasts, a positive correlation was only found between α-SMA in fibroblasts and SHH in OSCC tumor stroma ($p < 0.0001$, $\varphi = 0.51$) (Fig. 4). Higher in vitro protein expression of SHH and GLI-1 was observed in primary CAFs and NOFs. Although SHH was found to be localized in the cellular cytoplasm of both cell types, the GLI-1 transcription factor was present only in the nuclei of CAF (Fig. 5).

Discussion

The present results corroborate previously published evidence indicating that the HH pathway becomes reactivated through mediation by malignant and/or stromal cells, and also actively participate in the pathogenesis of OSCC (Cavicchioli Buim et al. 2011; Dias et al. 2016; Valverde et al. 2016; Takabatake et al. 2019). Our results also confirmed a heterogeneous immunophenotypic profile in the CAF populations studied herein, revealing that subpopulations of α-SMA + and S100A4 + CAFs were positive for the SHH ligand, as well as for GLI-1. While NOF cells were also positive for these ligands, no nuclear positivity for GLI-1 was observed. Accordingly, we hypothesize that these cells could be the source of the HH ligand and may mediate the paracrine activation of this cascade in malignant cells, or perhaps even by way of autocrine activation since GLI-1 was detected in the nuclei of CAFs.

Signaling pathways participating in embryonic development, such as the HH pathway, are maintained in an inactive state in adult tissues, and the reactivation of these has been associated with the development of several tumors (McMillan and Matsui 2012; Armas-López et al. 2017). In cancer, the HH pathway can be activated by HH ligand via the mutational activation of PTCH1 receptors, SMO, or even

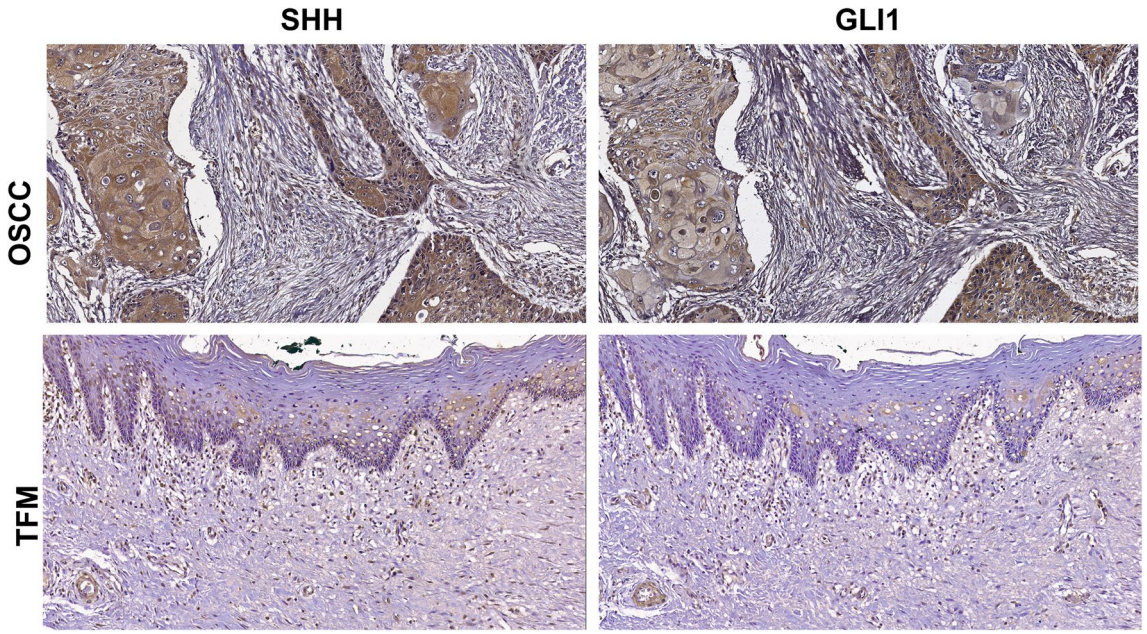

Fig. 3 Predominant HH molecule expression in OSCCs and TFMs. SHH and GLI1 (3 + score) in tumor islets (3 + score) and stroma (2 + score). SHH (1 + score) in the epithelium and lamina propria of TFM and GLI1 (1 + score) in the cytoplasm of epithelial cells and cells in the lamina propria of TFM. (Color figure online)

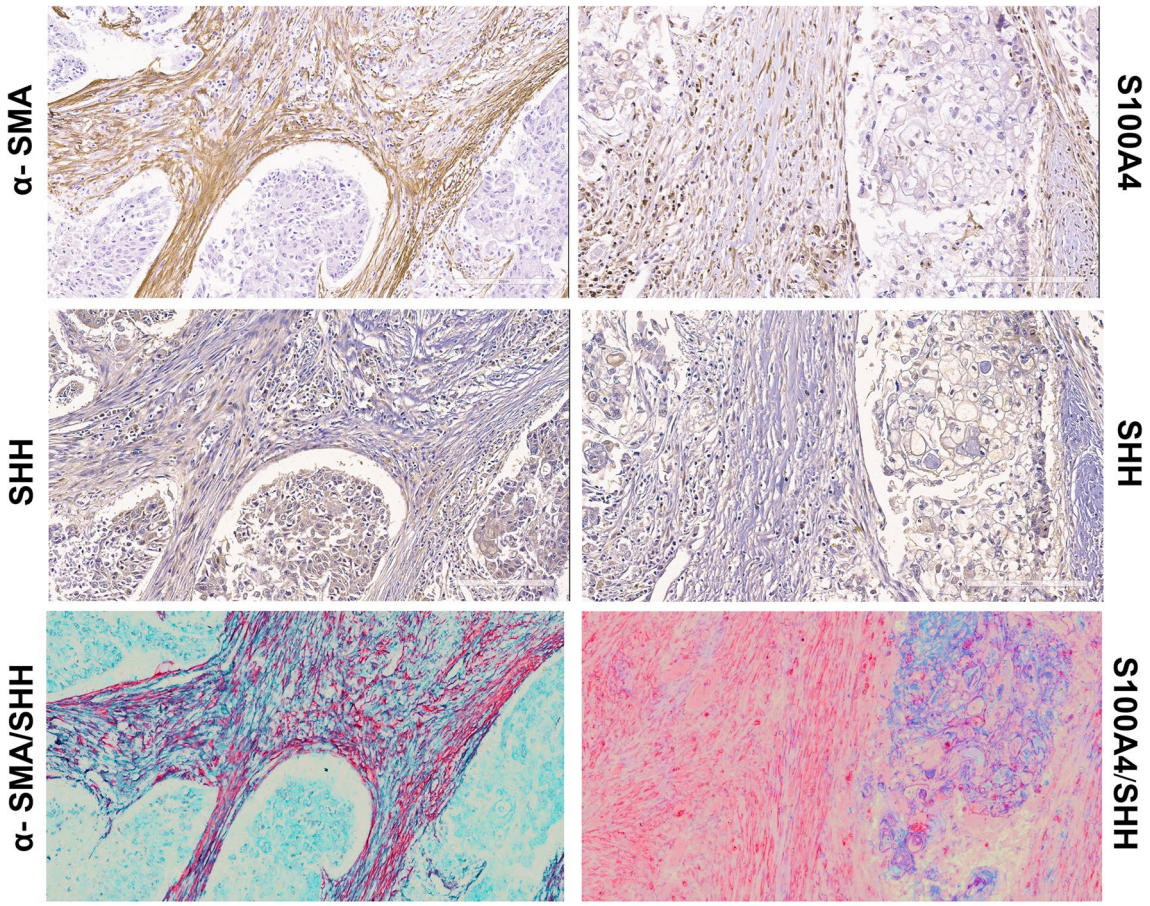

Fig. 4 Colocalization of SHH/α-SMA and SHH/S100A4. Immunoexpression of α-SMA in tumor stroma. Immunoexpression of SHH in malignant OSCC and tumor stroma. Double staining for α-SMA (Red Permanent) in stroma and SHH (Vina Green) in tumor islets and stroma, with colocalization of proteins α-SMA and SHH (purple) seen in tumor stroma. Immunoexpression of S100A4 in tumor stroma. Immunoexpression of SHH in OSCC tumor islets and stroma. Double staining for S100A4 in stroma (Red Permanent) and SHH in tumor islets (Vina Green). Colocalization of S100A4 and SHH (purple) seen in OSCC tumor cells. (Color figure online)

through increased GLI-1 levels, which can be mediated by other signaling pathways, such as TGFβ1. HH ligand may be secreted by tumor cells or in the tumor microenvironment, such as by CAF (Amakye et al. 2013; Gascard and Tlsty 2016). HH ligands have been reported to participate in the initiation and progression of tumors (Wu et al. 2017). For several years, the main focus of OSCC research was to study the participation of HH molecules in malignant cells, while the stroma has more recently been a major subject of investigation (Valverde et al. 2016; Valenti et al. 2017). The revelation that stromal cells, such as CAF, may be a source of HH ligands and may dynamically interact with the HH pathway, increases prospects for these cells' potential therapeutic role and highlights their participation in the pathogenesis of this signaling cascade in OSCC (Cavicchioli Buim et al. 2011; Valverde et al. 2016; Kuroda et al. 2017; Takabatake et al. 2019). CAFs are an important cell type in the context of stromal activation (Santi et al. 2018) and are involved in crosstalk between malignant and stromal cells (Hanahan and Coussens 2012). The role of activated fibroblasts in OSCC has been highlighted in recent decades, including evidence of the participation of α-SMA positive fibroblasts in the progression of OSCC (Lin et al., 2017; Santi et al, 2018; Ramos-Vega et al. 2020). The present study detected α-SMA expression exclusively in tumor stroma. This protein is highly indicative of activated fibroblast populations in several tumor types, such as breast (Orimo et al. 2005) and oral tumors (Kellermann et al. 2008; Sobral et al. 2011; Vered et al. 2019). α-SMA expression has been associated with an increased invasive potential (Kellermann et al. 2007, 2008; Sobral et al. 2011), and this α-SMA cell population has been correlated with the density of pro-tumor macrophages (Takahashi et al. 2017), which is another source of HH pathway ligand (Valverde et al. 2016).

Fibroblasts expressing S100A4 are also part of the OSCC CAF population, which serves to confirm the diverse origin of these cells (Kidd et al. 2012; Gascard and Tlsty 2016). More recent evidence indicates that S100A4 + cells represent

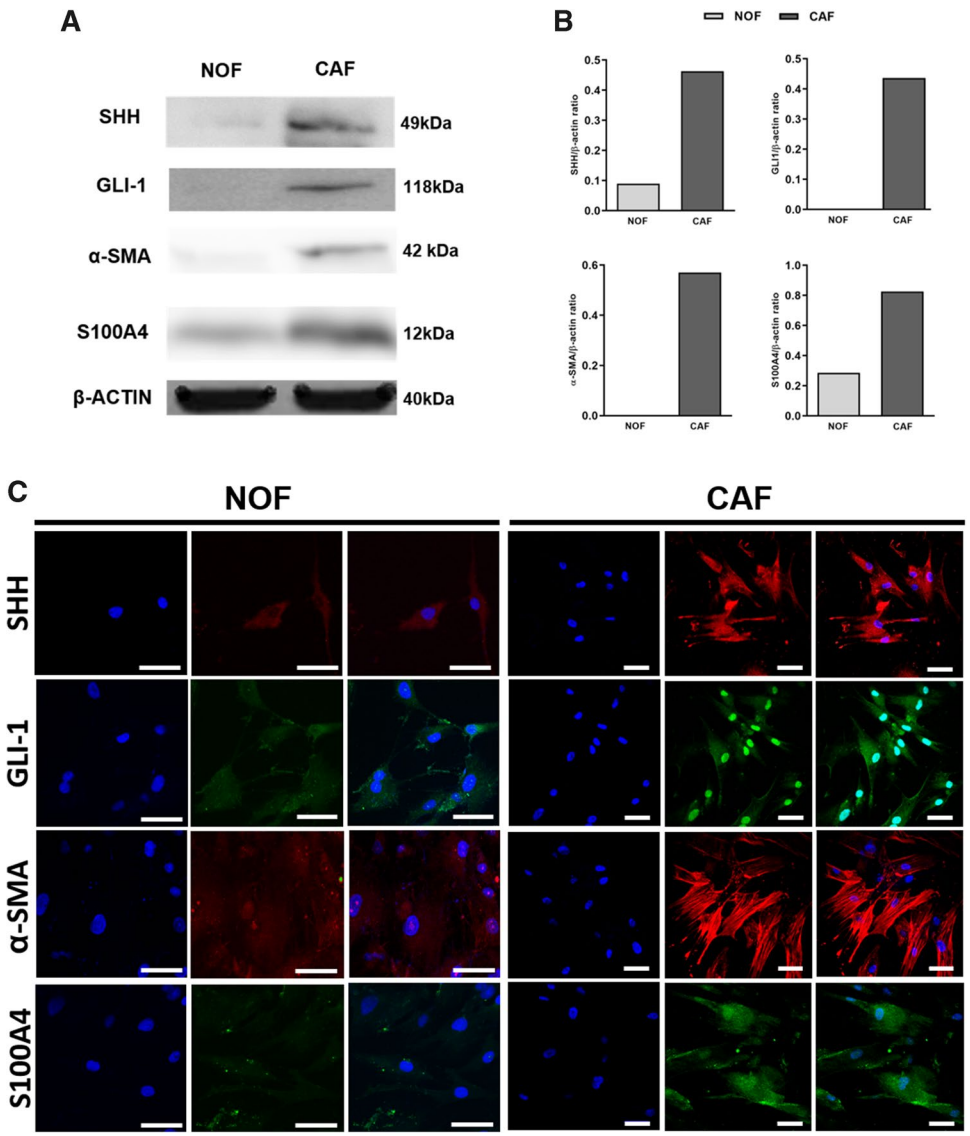

Fig. 5 **a** and **b** Western Blot analysis showing a higher expression of total SHH ligand, GLI1, α-SMA, and S100A4 proteins in CAFs. C) A higher cytoplasmic SHH expression and a unique nuclear GLI-1 expression in CAF compared to NOF. α-SMA and S100A4 markers were also more evident in CAFs. (Color figure online)

a population of quiescent, epigenetically stable fibroblasts considered to be precursors of activated fibroblasts (Kalluri 2016). In addition, S100A4 is expressed in malignant cells through the process of epithelial-mesenchymal transition (Öhlund et al. 2014; Gascard and Tlsty 2016), which may be coordinated by α-SMA + CAFs in OSCC (Zhou et al. 2014).

In the present study, immunostaining for S100A4 was also observed in the fibroblasts located in the lamina propria of TFMs, in contrast to α-SMA + CAF found exclusively in tumor stroma, indicating that α-SMA + is a suitable marker for determining CAF profile in OSCC (Sobral et al. 2011; Gascard and Tlsty 2016; Lin et al. 2017).

The presence of SHH detected herein in CAF and NOF cells isolated from OSCC and in human OSCC samples indicates that these cells are sources of HH ligand and may participate in the paracrine activation of the HH pathway in tumor cells (Valenti et al. 2017), as well as in other stromal cells (Abe and Tanaka 2016), including endothelial cells (Valverde et al. 2016). Since only α-SMA CAFs were found to express nuclear GLI-1, it follows that these cells may indeed be a source of HH ligands and could therefore participate in the paracrine and/or autocrine activation of this signaling cascade in malignant cells and CAFs, respectively. The fact that SHH was also observed in fibroblasts in TFM corroborates the crucial roles played by the HH ligand in promoting not only fibroblast proliferation and acting as a fibrogenic mitogen (Zhou et al. 2014), but also in inducing phenotypic transition into myofibroblasts (Horn et al. 2012; Zhou et al. 2014). As it remains unclear how the HH pathway influences fibroblast activation, this topic requires further research in the context of OSCC, especially considering the therapeutic potential of HH cascade components.

In the OSCC cases evaluated herein, SHH ligand immunoexpression in cancer cells seemed to be associated with

higher densities of α-SMA + CAFs, which indicates the possible participation of the HH pathway in the activation of α-SMA (Mpekris et al. 2017). In addition, the presence of nuclear GLI-1 in CAFs provides evidence of HH pathway activity in these cells, corroborating functional studies reporting that the presence of HH ligands enhances cellular proliferation rates (Bailey et al. 2008) and extracellular matrix deposition (Bailey et al. 2008; Valenti et al. 2017).

The present finding that α-SMA + CAFs express SHH suggests that HH signaling is important not only for cancer cell proliferation and activation, but also for the promotion of a microenvironment suitable for tumor development. In pancreatic cancer, inhibition of the HH pathway was shown to reduce the proliferation of CAFs, as well as tumor size (Mpekris et al. 2017). Accordingly, a recent study argued that the expression of HH molecules by CAFs may also be related to the activation of cellular programming favoring repair mechanisms and, consequently, the inhibition of tumor progression; however, this study focused on a specific type of bladder cancer (Shin et al. 2015).

In conclusion, the results presented here affirm the reactivation and participation of the HH pathway in OSCC and confirm the presence of a heterogeneous population of CAFs in this type of cancer. Herein we demonstrated the potential of CAFs as sources of HH ligands in OSCC. Both malignant and stromal cells were shown to secrete the SHH ligand, which is capable of not only mediating the hedgehog response in CAFs and stromal activation but also of promoting paracrine signaling in tumor and endothelial cells. We further observed a high density of CAFs adjacent to tumor islets, with enhanced SHH immunoexpression in OSCC. It follows that the inhibition of the HH pathway could result in suppressed tumor growth, either directly, by interfering with the survival of malignant cells, or indirectly, by altering the tumor microenvironment. Future studies should be conducted to more comprehensively investigate this topic.

Acknowledgements The authors thank Andris K. Walter for providing English translation and consulting services.

Funding The authors disclosed receipt of the following financial support for the research, authorship, and publication of this article: This work was supported by the National Council for Scientific and Technological Development (CNPq), [Grant No. 308595/2016-5].

Compliance with ethical standards

Conflict of interest The authors declare no conflict of interest.

References

Abe Y, Tanaka N (2016) The hedgehog signaling networks in lung cancer: the mechanisms and roles in tumor progression and implications for cancer therapy. Biomed Res Int. https://doi.org/10.1155/2016/7969286

Adrien J, Bertolus C, Gambotti L et al (2014) Why are head and neck squamous cell carcinoma diagnosed so late? influence of health care disparities and socio-economic factors. Oral Oncol 50:90–97. https://doi.org/10.1016/j.oraloncology.2013.10.016

Amakye D, Jagani Z, Dorsch M (2013) Unraveling the therapeutic potential of the Hedgehog pathway in cancer. Nat Med 19:1410–1422. https://doi.org/10.1038/nm.3389

Ansari SS, Sharma AK, Zepp M et al (2018) Upregulation of cell cycle genes in head and neck cancer patients may be antagonized by erufosine's down regulation of cell cycle processes in OSCC cells. Oncotarget 9:5797–5810. https://doi.org/10.18632/oncotarget.23537

Armas-López L, Zúñiga J, Arrieta O, Ávila-Moreno F (2017) The Hedgehog-GLI pathway in embryonic development and cancer: Implications for pulmonary oncology therapy. Oncotarget 8:60684–60703. https://doi.org/10.18632/oncotarget.19527

Bailey JM, Swanson BJ, Hamada T et al (2008) Sonic hedgehog promotes desmoplasia in pancreatic cancer. Clin Cancer Res 14:5995–6004. https://doi.org/10.1158/1078-0432.CCR-08-0291

Bray F, Ferlay J, Soerjomataram I (2018) Global cancer statistics 2018: GLOBOCAN estimates of incidence and mortality worldwide for 36 cancers in 185 countries. CA Cancer J Clin. https://doi.org/10.3322/caac.21492

Cavicchioli Buim ME, Gurgel CAS, Gonçalves Ramos EA et al (2011) Activation of sonic hedgehog signaling in oral squamous cell carcinomas: a preliminary study. Hum Pathol 42:1484–1490. https://doi.org/10.1016/j.humpath.2010.12.015

Cerami E, Gao J, Dogrusoz U et al (2012) The cBio cancer genomics portal: an open platform for exploring multidimensional cancer genomics data: figure 1. Cancer Discov 2:401–404. https://doi.org/10.1158/2159-8290.CD-12-0095

Chi AC, Day TA, Neville BW (2015) Oral cavity and oropharyngeal squamous cell carcinoma-an update. CA Cancer J Clin 65:401–421. https://doi.org/10.3322/caac.21293

Cirillo N, Hassona Y, Celentano A et al (2017) Cancer-associated fibroblasts regulate keratinocyte cell-cell adhesion via TGF-β-dependent pathways in genotype-specific oral cancer. Carcinogenesis 38:76–85. https://doi.org/10.1093/carcin/bgw113

Costea DE, Hills A, Osman AH et al (2013) Identification of two distinct carcinoma-associated fibroblast subtypes with differential tumor-promoting abilities in oral squamous cell carcinoma. Cancer Res 73:3888–3901. https://doi.org/10.1158/0008-5472.CAN-12-4150

Davis J (1971) Elementary survey analysis. Englewood cliffs. Prentice-Hall, NJ.

de FValverde L, de APereira T, Dias RB et al (2016) Macrophages and endothelial cells orchestrate tumor-associated angiogenesis in oral cancer via hedgehog pathway activation. Tumor Biol 37:9233–9241. https://doi.org/10.1007/s13277-015-4763-6

Dias RB, De Faro VL, Sales CBS et al (2016) Enhanced expression of hedgehog pathway proteins in oral epithelial dysplasia. Appl Immunohistochem Mol Morphol 24:596–602. https://doi.org/10.1097/PAI.0000000000000225

Dourado MR, Korvala J, Åström P et al (2019) Extracellular vesicles derived from cancer-associated fibroblasts induce the migration and invasion of oral squamous cell carcinoma. J Extracell Vesicles. https://doi.org/10.1080/20013078.2019.1578525

Gao J, Aksoy BA, Dogrusoz U et al (2013) Integrative analysis of complex cancer genomics and clinical profiles using the cBioPortal. Sci Signal. https://doi.org/10.1126/scisignal.2004088

Gascard P, Tlsty TD (2016) Carcinoma-associated fibroblasts: orchestrating the composition of malignancy. Genes Dev 30:1002–1019. https://doi.org/10.1101/gad.279737.116

Göritz C, Dias DO, Tomilin N et al (2011) A pericyte origin of spinal cord scar tissue. Science 333:238–242. https://doi.org/10.1126/science.1203165

Habib JG, O'Shaughnessy JA (2016) The hedgehog pathway in triple-negative breast cancer. Cancer Med 5:2989–3006. https://doi.org/10.1002/cam4.833

Hanahan D, Coussens LM (2012) Accessories to the crime: functions of cells recruited to the tumor microenvironment. Cancer Cell 21:309–322. https://doi.org/10.1016/j.ccr.2012.02.022

Horn A, Palumbo K, Cordazzo C et al (2012) Hedgehog signaling controls fibroblast activation and tissue fibrosis in systemic sclerosis. Arthritis Rheum 64:2724–2733. https://doi.org/10.1002/art.34444

IARC (2005) WHO histological classification of tumours of the oral cavity and oropharynx. In: Barnes L (ed) Pathology and genetics of head and neck tumours. IARC Press, France, pp 163–181

Jotzu C, Alt E, Welte G et al (2011) Adipose tissue derived stem cells differentiate into carcinoma-associated fibroblast-like cells under the influence of tumor derived factors. Cell Oncol 34:55–67. https://doi.org/10.1007/s13402-011-0012-1

Kalluri R (2016) The biology and function of fibroblasts in cancer. Nat Rev Cancer 16:582–598. https://doi.org/10.1038/nrc.2016.73

Kayamori K, Katsube KI, Sakamoto K et al (2016) NOTCH3 s induced in cancer-associated fibroblasts and promotes angiogenesis in oral squamous cell carcinoma. PLoS ONE 11:e0154112. https://doi.org/10.1371/journal.pone.0154112

Kellermann MG, Sobral LM, Da Silva SD et al (2007) Myofibroblasts in the stroma of oral squamous cell carcinoma are associated with poor prognosis. Histopathology 51:849–853. https://doi.org/10.1111/j.1365-2559.2007.02873.x

Kellermann MG, Sobral LM, da Silva SD et al (2008) Mutual paracrine effects of oral squamous cell carcinoma cells and normal oral fibroblasts: induction of fibroblast to myofibroblast transdifferentiation and modulation of tumor cell proliferation. Oral Oncol 44:509–517. https://doi.org/10.1016/j.oraloncology.2007.07.001

Kidd S, Spaeth E, Watson K et al (2012) Origins of the tumor microenvironment: quantitative assessment of adipose-derived and bone marrow-derived stroma. PLoS ONE. https://doi.org/10.1371/journal.pone.0030563

Kuroda H, Kurio N, Shimo T et al (2017) Oral squamous cell carcinoma-derived sonic hedgehog promotes angiogenesis. Anticancer Res 37:6731–6737

Lin NN, Wang P, Zhao D et al (2017) Significance of oral cancer-associated fibroblasts in angiogenesis, lymphangiogenesis, and tumor invasion in oral squamous cell carcinoma. J Oral Pathol Med 46:21–30. https://doi.org/10.1111/jop.12452

McMillan R, Matsui W (2012) Molecular pathways: the hedgehog signaling pathway in cancer. Natl Institutes Heal 18:4883–4888. https://doi.org/10.1158/1078-0432.CCR-11-2509

Mpekris F, Papageorgis P, Polydorou C et al (2017) Sonic-hedgehog pathway inhibition normalizes desmoplastic tumor microenvironment to improve chemo- and nanotherapy. J Control Release 261:105–112. https://doi.org/10.1016/j.jconrel.2017.06.022

Nayak A, Siddharth S, Das S et al (2017) Nanoquinacrine caused apoptosis in oral cancer stem cells by disrupting the interaction between GLI1 and β catenin through activation of GSK3β. Toxicol Appl Pharmacol 330:53–64. https://doi.org/10.1016/j.taap.2017.07.008

Öhlund D, Elyada E, Tuveson D (2014) Fibroblast heterogeneity in the cancer wound. J Exp Med 211:1503–1523. https://doi.org/10.1084/jem.20140692

Orimo A, Gupta PB, Sgroi DC et al (2005) Stromal fibroblasts present in invasive human breast carcinomas promote tumor growth and angiogenesis through elevated SDF-1/CXCL12 secretion. Cell 121:335–348. https://doi.org/10.1016/j.cell.2005.02.034

Otsuka A, Levesque MP, Dummer R, Kabashima K (2015) Hedgehog signaling in basal cell carcinoma. J Dermatol Sci 78:95–100. https://doi.org/10.1016/j.jdermsci.2015.02.007

Peiris-Pagès M, Sotgia F, Lisanti M (2015) Chemotherapy induces the cancer-associated fibroblast phenotype, activating paracrine Hedgehog-GLI signalling in breast cancer cells. Oncotarget 6:10728–10745. https://doi.org/10.18632/oncotarget.3828

Quante M, Tu SP, Tomita H et al (2011) Bone marrow-derived myofibroblasts contribute to the mesenchymal stem cell niche and promote tumor growth. Cancer Cell 19:257–272. https://doi.org/10.1016/j.ccr.2011.01.020

Ramos-Vega V, Venegas Rojas B, Donoso Torres W (2020) Immunohistochemical analysis of cancer-associated fibroblasts and podoplanin in head and neck cancer. Med Oral Patol Oral y Cir Bucal. https://doi.org/10.4317/medoral.23335

Santi A, Kugeratski FG, Zanivan S (2018) Cancer associated fibroblasts: the architects of stroma remodeling. Proteomics 18:1–15. https://doi.org/10.1002/pmic.201700167

Shin K, Lim A, Zhao C et al (2015) Hedgehog signaling restrains bladder cancer progression by eliciting stromal production of urothelial differentiation factors. Cancer Cell 26:521–533. https://doi.org/10.1016/j.ccell.2014.09.001.Hedgehog

Sobral LM, Bufalino A, Lopes MA et al (2011) Myofibroblasts in the stroma of oral cancer promote tumorigenesis via secretion of activin A. Oral Oncol 47:840–846. https://doi.org/10.1016/j.oraloncology.2011.06.011

Spivak-Kroizman TR, Hostetter G, Posner R et al (2013) Hypoxia triggers hedgehog-mediated tumor-stromal interactions in pancreatic cancer. Cancer Res 73:3235–3247. https://doi.org/10.1158/0008-5472.CAN-11-1433

Takabatake K, Shimo T, Murakami J et al (2019) The role of sonic hedgehog signaling in the tumor microenvironment of oral squamous cell carcinoma. Int J Mol Sci. https://doi.org/10.3390/ijms20225779

Takahashi H, Sakakura K, Kudo T et al (2017) Cancer-associated fibroblasts promote an immunosuppressive microenvironment through the induction and accumulation of protumoral macrophages. Oncotarget 8:8633–8647. https://doi.org/10.18632/oncotarget.14374

The World Health Organization (2001) Declaration of Helsinki: World medical association Declaration of Helsinki. Bull world Heal Organ 79:373–374

Theunissen JW, de Sauvage FJ (2009) Paracrine hedgehog signaling in cancer. Cancer Res 69:6007–6010. https://doi.org/10.1158/0008-5472.CAN-09-0756

Valenti G, Quinn HM, Heynen GJJE et al (2017) Cancer stem cells regulate cancer-associated fibroblasts via activation of hedgehog signaling in mammary gland tumors. Cancer Res 77:2134–2147. https://doi.org/10.1158/0008-5472.CAN-15-3490

Vered M, Shnaiderman-Shapiro A, Zlotogorski-Hurvitz A et al (2019) Cancer-associated fibroblasts in the tumor microenvironment of tongue carcinoma is a heterogeneous cell population. Acta Histochem 121:151446. https://doi.org/10.1016/j.acthis.2019.151446

Wu F, Zhang Y, Sun B et al (2017) Hedgehog signaling: from basic biology to cancer therapy. Cell Chem Biol 24:252–280. https://doi.org/10.1016/j.chembiol.2017.02.010

Zhou B, Chen WL, Wang YY et al (2014) A role for cancer-associated fibroblasts in inducing the epithelial-to-mesenchymal transition in human tongue squamous cell carcinoma. J Oral Pathol Med 43:585–592. https://doi.org/10.1111/jop.12172